Automated classification of ICA networks from resting state fMRI using Machine Learning framework

Ashish Anil Rao[1], Hima Patel[1], Ek Tsoon Tan[2], Rakesh Mullick[1], and Suresh Emmanuel Joel[1]
[1]General Electric Global Research, Bangalore, Karnataka, India, [2]General Electric Global Research, New York, United States

Introduction: Independent component analysis (ICA) has been widely used to extract functional networks from resting state functional MRI (rs-fMRI) [1]. Among all the independent components (ICs) generated, some are of neurophysiological origin ("good"), while others arise due to physiological and system noise ("bad"). It is often of interest to separate neuronal networks from noise. Labeling components is typically performed manually by experts and is tedious, subjective and error prone. Clinical feasibility of ICA is also limited by the need for manual extraction of functional networks. Automatic classification of the ICs into good or bad networks will alleviate these problems. Previous approaches that have addressed this problem with modest results include template matching for DMN [2], supervised classification based on a global decision tree classifier [3], IC-fingerprint combined with SVM classifier [4], CORSICA [5] and FENICA [6]. More recently, a tool named FIX using FSL has been reported to perform automatic classification for high dimensional ICA from high resolution, long duration multiband connectome data [7]. Here, we present a clinically feasible automated classification method for ICA components obtained from classical non-multiband short duration rs-fMRI acquisition on single subjects. Several spatial and temporal features were extracted from the ICs and fed to a random forests classifier for training and testing. Sensitivity and specificity of 92% was obtained based on single subject short duration rs-fMRI.

Methods: For each of 10 participants, 10 runs of resting state fMRI (7 minute long, TR/TE=2000/30 ms, FA = 75°, 3 mm isotropic voxel with 1 mm slice gap) were obtained using a GE Discovery 750 3T MR scanner. A T1-weighted image was also acquired for normalization to atlas. The data were slice time corrected, motion corrected, coregistered, spatially transformed to MNI space, spatially smoothed and nuisance removed (by regressing motion parameters, global signal, top 90% of WM and CSF signal using PCA, COMPCOR, [8]). 10 group ICAs, one for each participant (all 10 runs) with temporal concatenation was performed using a custom developed implementation of spatial ICA. 40 ICs were obtained (based on MDL criterion [9]) and back reconstructed to give time courses and spatial maps for each participant and each run. Several features were generated for each back reconstructed IC. The power spectrum of the time course was computed and the ratio of the average low frequency (<0.1Hz) power to the average high frequency (>0.1Hz) power was calculated as a feature. Spatial similarity was computed using correlation coefficient with a locally developed functional atlas (using independent data) as the next set of features. Correlation coefficient with a brain stem mask, and probabilistic WM and CSF masks was the final set of features. Ground truth (GT) (labeling ICs as good or bad) was done by visual inspection by experts. The 4000 back-reconstructed ICs (40 components, 10 participants, 10 runs) along with their GT labels and features were supplied to a machine learning framework implemented as a random forest classifier. 80% of the data (3200 components from 80 runs from 8 random participants) were used for training and 20% (the remaining 800 components from 20 runs from 2 participants) for testing. The good/bad labels obtained from the random forests classifier on the testing data were compared with the GT labels and sensitivity, specificity and accuracy were computed. The flowchart of the pipeline for processing the data is illustrated in Fig 1.

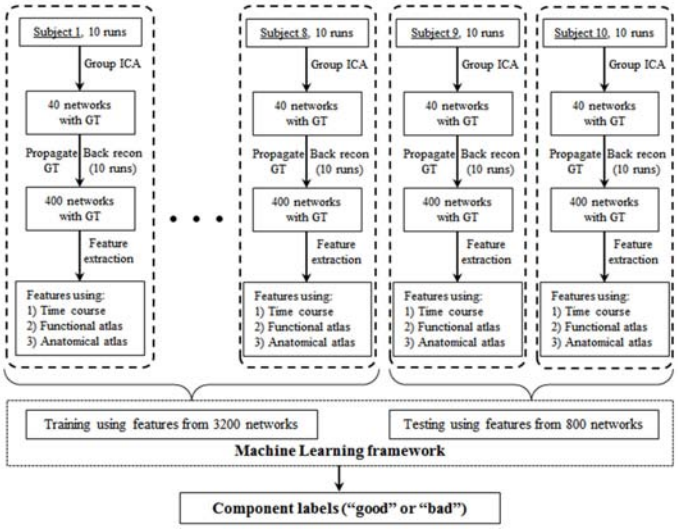

Figure 2: Flowchart of processing pipeline

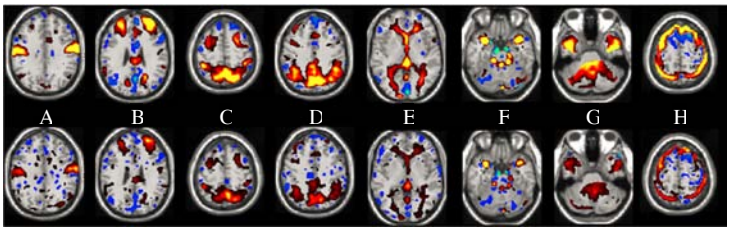

Figure 1: Examples of typical "good" (A-D) and "bad" (E-H) components obtain using ICA at the group level (top row) and the back reconstructed individual subject and run level (bottom row).

Results and Discussion: Fig 2 illustrates four good and four bad networks at group level as well as back reconstructed individual subject and run level. With leave two-subject out method, the classifier's accuracy was 92% (sensitivity of 92% and specificity of 92%), i.e. on a typical 30 or 40 component ICA, an average of 3 could be classified incorrectly. In our method, the ground truth was generated using single-subject group analysis (one group = 1 subject 10 runs) and the classifier was trained and tested on back-reconstructed ICA components (1 subject 1 run). This was done because it was difficult to generate ground truth from single subject single run ICA's due to ambiguity (difficulty to classify a network) and tediousness (visualizing and marking 4000 networks). When the errors in classification were investigated, even "experts" could not classify some of those networks with confidence. Most accurately classified functional networks were visual, default mode, motor, executive, and control networks. The networks that were most often incorrectly classified were the anterior default mode network (very similar to orbitofrontal cortex (OFC) susceptibility artefact noise component) and superior sensorimotor network (very similar to cap-like motion artefact component).

Conclusions: Our classifier has to potential to work sufficiently well on single-subject single-session making it clinically useful. It could be used for automatic extraction of functional networks and for automated denoising of fMRI data by reconstructing data after removing "bad" components.

References: [1] McKeown MJ et al., 1998, HBM, 6(3), 160-88. [2] Greicius MD et al., 2004, PNAS, 101(13), 4637-4642. [3] Tohka J et al., 2008, Neuroimage, 39(3), 1227-1245. [4] De Martino F et al., 2007, Neuroimage, 34(1), 177-194. [5] Perlbarg V et al., 2007, MRI, 25(1), 35-46. [6] Schöpf V et al., 2010, J Neurosci Methods, 192(2), 207-213. [7] Smith SM et al, 2013, Neuroimage, 80, 144-168. [8] Behzadi Y et al, 2007, NeuroImage, 37(1), 90-101. [9] Li YO et al., 2007, HBM, 28(11), 1251-1266.